Available online at www.sciencedirect.com
ScienceDirect
International Journal of Thermal Sciences 47 (2008) 369–377
International Journal of Thermal Sciences
www.elsevier.com/locate/ijts

Natural convection in an open square cavity with discrete heaters at their optimized positions

A. Müftüoğlu, E. Bilgen *

Ecole Polytechnique, Box 6079, centre ville, Montreal, QC, H3C 3A7, Canada

Received 9 January 2007; received in revised form 27 March 2007; accepted 28 March 2007

Available online 23 May 2007

Abstract

In this article, we determined optimum positions of discrete heaters by maximizing the conductance and then studied heat transfer and volume flow rate with discrete heaters at their optimum positions. Continuity, Navier–Stokes and energy equations are solved by finite difference – control volume numerical method. The relevant governing parameters were: the Rayleigh numbers, Ra from 10^3 to 10^7, the cavity aspect ratio, $A = H/L = 1$, the heater size h/L from 0.05 to 0.20 and number of heaters from 1 to 3. We found that the global conductance is as an increasing function of the Rayleigh number, the heater size and the number of heaters. Best thermal performance is obtained by positioning the discrete heaters closer to the bottom and closer to each other at the beginning of fluid flow. The configuration is not equidistance but follows a function of the Rayleigh number. The Nusselt number and the volume flow rate in and out the open cavity are also increasing functions of the Rayleigh number, the heater size and the number of heaters.

Keywords: Natural convection; Square open cavity; Discrete heat sources; Constructal method; Optimum heaters position

1. Introduction

The thermal performance of electronic packages containing a number of discrete heat sources has been studied extensively in the literature. The design problem in electronic packages is to maintain cooling of chips in an effective way to prevent overheating and hot spots. This is achieved generally by effective cooling by natural convection, mixed convection and in certain cases by other means such as heat pipes, and finally by better design. In the latter case, the objective is to maximize heat transfer density so that the maximum temperature specified for safe operation of a chip is not exceeded. Thus, optimum placement of discrete heaters with respect to usual equidistant placement may be required. In this respect, few theoretical and experimental studies have been published (e.g. [1–3]). As an application of the constructal method, an analytical study has been presented by da Silva et al. [3] for the case of large number of heat sources placed on a vertical plate. As expected, it is shown that the heaters should be placed closer when they are placed at the beginning of cooling fluid flow and further apart later when in contact with already heated cooling fluid flow. Recently, several papers on various geometrical configurations have been published on optimal distribution of discrete heaters over a horizontal plate with laminar forced convection [4] and in open ended channels with natural convection [5–7].

We see from the brief review that the case of open cavities with discrete heaters in their optimum positions has not been addressed in the literature. In the present study, our aim is (i) To determine optimum positions of small number of discrete heaters with finite size placed on the vertical wall facing the opening of an open square cavity. The discrete heaters are cooled by the ambient air circulating through the opening. (ii) To study the thermal performance of optimally placed heaters in a square open cavity.

2. Problem and mathematical model

The problem is to determine the optimum position of one, two or more discrete heating elements in an open square cav-

* Corresponding author. Tel.: +1 (514) 340 4711 ext. 4579; fax: +1 (514) 340 5917.
E-mail address: bilgen@polymtl.ca (E. Bilgen).

1290-0729/$ – see front matter
doi:10.1016/j.ijthermalsci.2007.03.015

Nomenclature

A	enclosure aspect ratio, $= H/L$
c_p	heat capacity ..... J/kg K
g	acceleration due to gravity ..... m/s^2
H	cavity height ..... m
h	heater size ..... m
k	thermal conductivity ..... W/m K
L	cavity width ..... m
Nu	Nusselt number, defined by Eq. (6)
n	coordinate in any direction
p	pressure ..... Pa
P	dimensionless pressure, $= (p - p_\infty)L^2/\rho\alpha^2$
Pr	Prandtl number, $= \upsilon/\alpha$
q''	heat flux ..... W/m^2
q	dimensionless heat flux, $= \frac{\partial\theta}{\partial X}$
Ra	Rayleigh number, $= g\beta q'' L^4/(\upsilon\alpha k)$
T	temperature ..... K
t	time ..... s
U, V	dimensionless fluid velocities, $= uL/\alpha, vL/\alpha$
$\dot{V}$	dimensionless volume flow rate through the opening
X, Y	dimensionless Cartesian coordinates, $= x/L, y/L$
x, y	Cartesian coordinates

Greek symbols

α	thermal diffusivity ..... m^2/s
β	volumetric coefficient of thermal expansion .. 1/K
υ	kinematic viscosity ..... m^2/s
ρ	fluid density ..... kg/m^3
ψ	stream function
θ	dimensionless temperature, $= (T - T_\infty)/(Lq''/k)$
τ	dimensionless time, $= \alpha t/L^2$

Superscripts

$-$	average

Subscripts

ext	extremum
in	into cavity
max	maximum
opt	optimum
∞	ambient value
1, 2, 3	first, second and third heater

ity, cooled by natural convection. Further, heat transfer performance of each case is studied using the determined optimum positions.

Schematic of the two-dimensional open square cavity with three discrete heating elements case and the boundary conditions are shown in Fig. 1. All three solid boundaries of the cavity are adiabatic and the side facing the vertical left boundary is open to ambient air. One, two or three discrete heating elements are installed on the vertical left boundary. Each heating element of height h and coordinate $(0, y_i)$ dissipates heat at constant heat flux, q''. The cooling air from a reservoir enters the cavity through the lower part of the opening; it circulates along the heating elements and exits from the upper part of the opening.

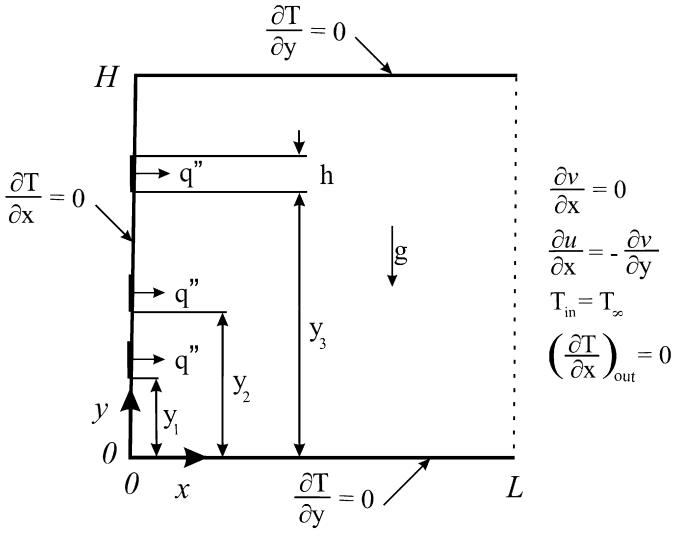

Fig. 1. Schematic of the square cavity, the coordinate system and boundary conditions.

Two-dimensional conservation equations for mass, momentum and energy are used with Bussinesq approximation. It is assumed that the radiation is negligible. By using L as the length scale, α/L as the velocity scale, Lq''/k as the temperature scale and L^2/α for the time scale, we obtained following non-dimensional equations

$$\frac{\partial U}{\partial X} + \frac{\partial V}{\partial Y} = 0 \tag{1}$$

$$\frac{\partial U}{\partial \tau} + U\frac{\partial U}{\partial X} + V\frac{\partial U}{\partial Y} = -\frac{\partial P}{\partial X} + Pr\nabla^2 U \tag{2}$$

$$\frac{\partial V}{\partial \tau} + U\frac{\partial V}{\partial Y} + V\frac{\partial V}{\partial Y} = -\frac{\partial P}{\partial Y} + Ra\,Pr\,\theta + Pr\,\nabla^2 V \tag{3}$$

$$\frac{\partial \theta}{\partial \tau} + U\frac{\partial \theta}{\partial X} + V\frac{\partial \theta}{\partial Y} = \nabla^2\theta \tag{4}$$

where $Ra = g\beta q'' L^4/(\upsilon\alpha k)$ and $Pr = \upsilon/\alpha$.

The average and normalized Nusselt numbers are calculated as

$$\overline{Nu} = \frac{-\int_0^A \frac{\partial\theta}{\partial X}\,dY}{\int_0^A (\theta_1 - \theta_2)} \tag{5}$$

$$Nu = \frac{\overline{Nu}_{Ra}}{\overline{Nu}_{Ra=0}} \tag{6}$$

where $\overline{Nu}_{Ra=0}$ is calculated at $Ra = 0$.

The volume flow rate, $\dot{V}$ is calculated as

$$\dot{V} = -\int_{X=1} U_{\text{in}}\,dY \tag{7}$$

where $U_{\text{in}} = U_{X=1}$ if $U_{X=1} < 0$ and $U_{\text{in}} = 0$ if $U_{X=1} \geqslant 0$.

The stream function is calculated from its definition as

$$U = -\frac{\partial \psi}{\partial Y}, \qquad V = \frac{\partial \psi}{\partial X} \tag{8}$$

ψ is zero on the solid surfaces and the streamlines are drawn by $\Delta\psi = (\psi_{\max} - \psi_{\min})/n$ with n is the number of increments.

Boundary conditions are

$$\text{On solid surfaces:} \quad U = 0,\ V = 0 \tag{9}$$

$$\text{On adiabatic walls:} \quad \frac{\partial \theta}{\partial n} = 0 \tag{10}$$

$$\text{On the heaters:} \quad q = \frac{\partial \theta}{\partial X} = 1 \tag{11}$$

$$\text{At the opening:} \quad \frac{\partial V}{\partial X} = 0,\ \frac{\partial U}{\partial X} = -\frac{\partial V}{\partial Y}$$
$$\left(\frac{\partial \theta}{\partial X}\right)_{\text{out}} = 0,\ \theta_{\text{in}} = 0 \tag{12}$$

The boundary condition at the opening, Eq. (12) is shown to be a satisfactory for the case of computation domain confined to the open cavity [8].

The conductance is calculated as

$$C = \frac{\int_y^{y+h} q' \,\mathrm{d}y}{k(T_{\max} - T_\infty)} = \frac{h/L}{\theta_{\max}} \tag{13}$$

3. Numerical technique

The numerical method used to solve Eqs. (1) to (4) with the boundary conditions Eqs. (8) to (11) is the SIMPLER (Semi-Implicit Method for Pressure Linked Equations Revised) algorithm [9]. The computer code based on the mathematical formulation presented above and the SIMPLER method were validated earlier with respect to the benchmark [10]. The results of validation with the benchmark [11] as well as another [12] showed that the deviations in Nusselt number and the maximum stream function at $Ra = 10^6$ were 0.60% and 1.12% respectively. It was seen that the concordance was excellent. In addition, the average Nusselt numbers at the hot and cold walls were compared, which showed a maximum difference of about 0.5% in all runs. The present code was tested also to simulate the case studied by Chan and Tien with enlarged computational domain [13]. We used restricted computational domain and compared the results with theirs with extended computational domain. The results are shown in Table 1. It is noted that in restricted domain case, the deviation is higher at $Ra = 10^7$, because the flow simulation at the cavity corners is not perfect. Despite this, the approximation made is acceptable.

Uniform grid in X and Y direction were used for all computations. Grid convergence was studied for the case of $A = 1$ with grid sizes from 21×21 to 151×151 at $Ra = 10^5$ and 10^7. The results are presented in Table 2. We see in the 5th and 6th columns that, the variations in Nu and C are 6.2×10^{-4} and 1.07×10^{-2} respectively at $Ra = 10^5$, and they are 2.1×10^{-3} and 1.3×10^{-2} respectively at $Ra = 10^7$. Hence, we made a compromise between computation time and precision, and selected the grid size of 81×81. Using a system with a processor of 3.2 GHz clock speed, for $A = 1$, 81×81 grid size, at $Ra = 10^6$, the typical execution time was 92 s for single heater case and 76 s for three heaters case.

Table 1
Comparison of the results with the enlarged domain [13] and the cavity restricted domain used in this study

Ra	$Nu/\dot{V}$ [13]	$Nu/\dot{V}$ [this study]	% Deviations
10^5	7.69/21.10	7.81/22.65	−1.56/−7.34
10^6	15.00/47.30	15.23/47.02	−1.53/+0.59
10^7	28.60/96.00	29.86/94.15	−4.41/+1.93

Table 2
Grid independence study results with $A = 1$ at $Ra = 10^5$ and 10^7

Size		21×21	41×41	61×61	81×81	101×101	151×151
$Ra = 10^5$	Nu	3.323	3.223	3.211	3.206	3.204	3.201
	C	0.818	0.940	0.985	1.008	1.021	1.039
$Ra = 10^7$	Nu	6.973	6.918	6.831	6.800	6.786	6.773
	C	1.287	1.592	1.672	1.709	1.733	1.766

A converged solution was obtained by iterating in time until variations in the primitive variables between subsequent time steps were:

$$\sum \left(\phi_{i,j}^{\text{old}} - \phi_{i,j}\right) < 10^{-4} \tag{14}$$

where ϕ stands for U, V, and θ.

Within the same time step, the residual of the pressure term was less than 10^{-3} [9]. In addition, the accuracy of the solution was double-checked using the energy conservation on the domain to ensure it was less than 10^{-4}.

4. Results and discussion

In the first part, we present the optimization study results and in the second, a parametric study results obtained with the discrete heating elements at their optimum positions. The aspect ratio was, $A = 1$ and kept constant. The variable parameters considered are dimensionless height of heating element, $h/L = 0.05$, 0.10 and 0.20, number of heating elements, $N = 1$, 2 and 3, and Rayleigh number, $Ra = 10^3$ to 10^7. Prandtl number, $Pr = 0.71$ for air was kept constant.

4.1. Optimization study

It was carried out to obtain the optimum position of heating elements by taking the number of heaters and their size constant, and by varying their positions. The procedure was as follows: (i) We compute conductance $C(Y)$ for a given N and h/L, at a constant Ra, (ii) we determine the maximum conduction, $C_{\max}$ at its optimum position Y_{opt}. (iii) We repeat the steps (i) and (ii) to determine $C(Y)$, $C_{\max}$ and Y_{opt} at all the other Rayleigh numbers, from 10^3 to 10^7, while keeping N and h/L the same. (iv) We repeat the steps (i) and (iii) to obtain the maximum conductance at its optimum position, $C_{\max}(Y_{\text{opt}})$ for the same number of heater, N but different heater sizes, h/L. Then, we repeat the steps (i)–(iv) to obtain the maximum conductance at its optimum position, $C_{\max}(Y_{\text{opt}})$ for different number of heaters, N. With the variable parameters considered above,

for each heater size, we had 80 computations for $N = 1$, 250 for $N = 2$ and 190 for $N = 3$. For three heater sizes, we had all together about 1500 computations to determine the optimum positions of the cases studied.

Typical results to obtain the conductance $C(Y)$ for $N = 1$, $h/L = 0.10$, $Ra = 10^3$, 10^5 and 10^7 are presented in Fig. 2(a). We can make several observations: (i) For all the Rayleigh numbers, the conductance changes with the position of the heater. We have smaller conductance at the lowest position when the heater is at the bottom; the conductance is increasing gradually as its position is raised reaching a maximum around mid-height and it is decreasing thereafter to another low conductance at the top position. This is expected since the cold air enters the cavity from the bottom, flows over the lower horizontal boundary and turns around before reaching the vertical side; hence, the conductance is lower near the bottom corner. As the heater is positioned higher, the incoming cold air flows over it; its conductance increases and reaches its maximum value at its optimum position. At the near top position, the air flow is again turned away from the heater to follow the top horizontal boundary and exit the cavity; hence the conductance is again relatively lower. (ii) For all cases, we see broad maxima, though using the computation results or changing scale of conductance, it is not difficult to identify $C_{\max}$ at its Y_{opt}. (iii) As the Rayleigh number is increased, the air flow as well as the conductance is increased. Following the increased air flow rate and resulting streamlines, the conductance, $C(Y)$ is increased accordingly. Indeed, ψ_{ext} and $\theta_{\max}$ are 0.414 and 0.1905 at $Ra = 10^3$, 5.4799 and 0.1019 at $Ra = 10^5$ and 18.9763 and 0.0492 at $Ra = 10^7$. They show that as Ra is increased, the circulation is increased and the maximum temperature is decreased, which is an expected result.

The effect of the heater size for $Ra = 10^6$ is presented in Fig. 2(b) for $h/L = 0.05$, 0.10 and 0.20. We see that the conductance is strongly affected by the heater size. In fact, ψ_{ext} and $\theta_{\max}$ are both increasing functions of the heater size. For example, at $Y = 0.5$, ψ_{ext} and $\theta_{\max}$ are 9.0116 and 0.0524 for $h/L = 0.05$, 10.7295 and 0.0701 for $h/L = 0.10$ and 12.4927 and 0.0904 for $h/L = 0.20$. Thus, the conductance calculated by Eq. (13) is $C = 0.95$, 1.43 and 2.21 for $h/L = 0.05$, 0.10 and 0.20 respectively.

We present streamlines and isotherms in Fig. 3 for the cases corresponding to Fig. 2(a) at $Ra = 10^3$, 10^5 and 10^7. The heater size is $h/L = 0.10$ and its two positions are shown, the upper figures at the bottom, $Y = 0$ and the lower ones are at the optimum position. We observe in Fig. 3(a) at $Ra = 10^3$ that the heat transfer is conduction dominated and the flow in both cases is almost similar, the flow is affected by the heater and it is slightly non-symmetric. ψ_{ext} and $\theta_{\max}$ for $Ra = 10^3$ are 0.3992 and 0.2547 at $Y = 0$ and 0.4141 and 0.1895 at $Y = Y_{\text{opt}}$. It is seen that the heater at its optimum position is better cooled by the inflowing air. At $Ra = 10^5$ in Fig. 3(b), ψ_{ext} and $\theta_{\max}$ are 6.1484 and 0.1538 at $Y = 0$ and 5.6808 and 0.0992 at $Y = Y_{\text{opt}}$. Again, the cooling is better at $Y = Y_{\text{opt}}$ position. Finally, at $Ra = 10^7$ in Fig. 3(c), ψ_{ext} and $\theta_{\max}$ are 25.7182 and 0.0585 at $Y = 0$ and 20.5515 and 0.0491 at $Y = Y_{\text{opt}}$. Once again, the cooling is better at $Y = Y_{\text{opt}}$. Thus, Fig. 3 shows that our observations regarding Fig. 2(a) are confirmed.

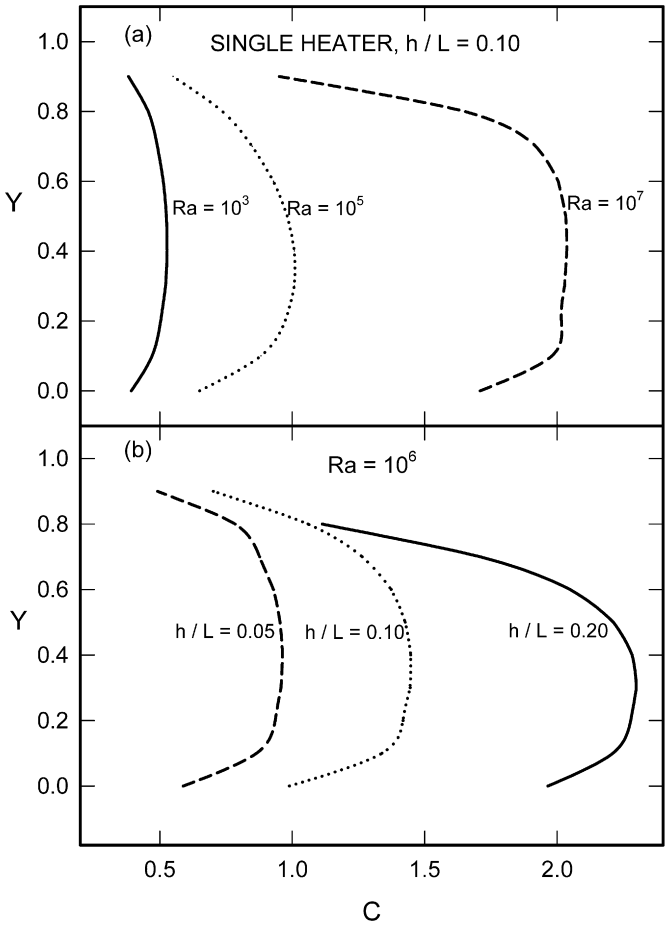

Fig. 2. The maximization of the global conductance when only one heat source is present.

We present in Fig. 4 (a) and (b) the optimum heater position Y_{opt} and the maximum conductance $C_{\max}$ as a function of the Rayleigh number for a single heater having $h/L = 0.05$, 0.10 and 0.20. We see in Fig. 4(a) that generally, the optimum position is slightly decreasing function of the Rayleigh number; this is expected since for increasing Ra, the circulation increases at the lower half of the cavity and the optimum heater position is at slightly lower level. We see also that Y_{opt} is at a lower position as the heater size is increased, as observed earlier in Fig. 2. We see in Fig. 4(b) that the maximum conductance $C_{\max}$ is an increasing function of the Rayleigh number, as observed in Fig. 2(a). $C_{\max}$ is an increasing function of heater size, as a consequence of our observations in Fig. 2(b). The results of Fig. 4 show that the optimum position of a single heater is at the lower half of the open cavity and not at the center. The conductance is maximized by lowering Y_{opt} slightly as the Rayleigh number is increased.

Following the procedure outlined earlier, we studied the cases with two heaters and three heaters. For two heaters case, the optimum position Y_{opt} is determined by searching the best position of the second heater while keeping the first at a fixed position and then repeating this procedure until all position

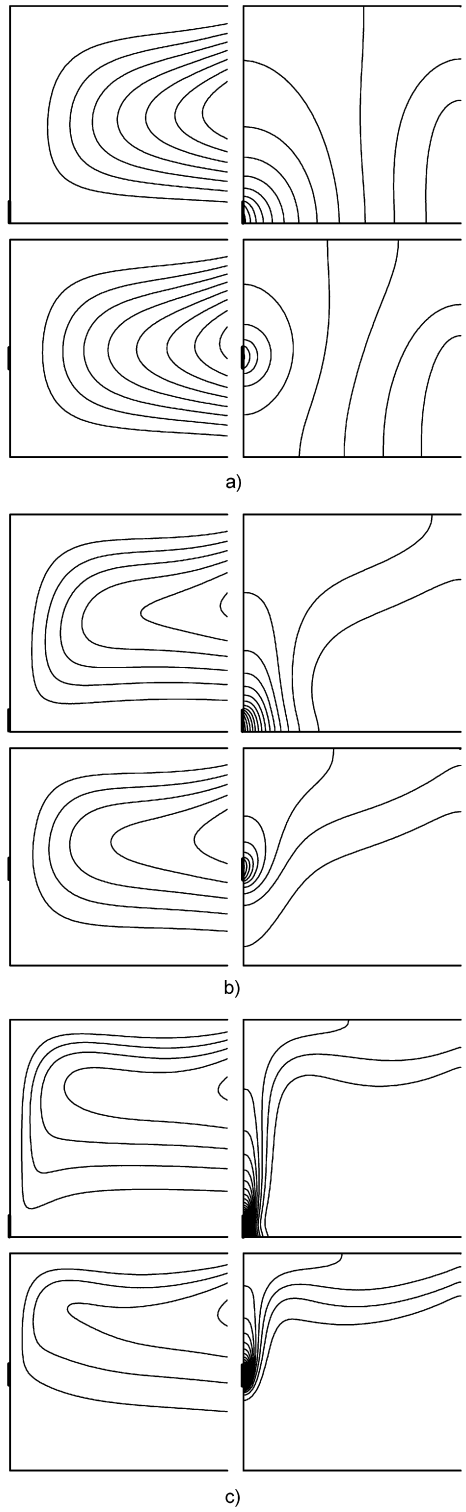

Fig. 3. Streamlines (on the left) and isotherms (on the right) for $h/L = 0.10$, the most lower heater position (the upper figure), the optimum heater position (the lower figure, (a) $Ra = 10^3$, Y_{opt} (the upper and lower figure) = 0.0 and 0.41, (b) $Ra = 10^5$, Y_{opt} (the upper and lower figure) = 0.0 and 0.39, (c) $Ra = 10^7$, Y_{opt} (the upper and lower figure) = 0.0 and 0.38.

combinations are obtained. As a result, the global maximum conductance C_{max} for the two heaters is found. The results are shown in Fig. 5. We see in Fig. 5(a) that the trends for both heaters are similar to the case of the single heater, i.e., Y_{opt} is a

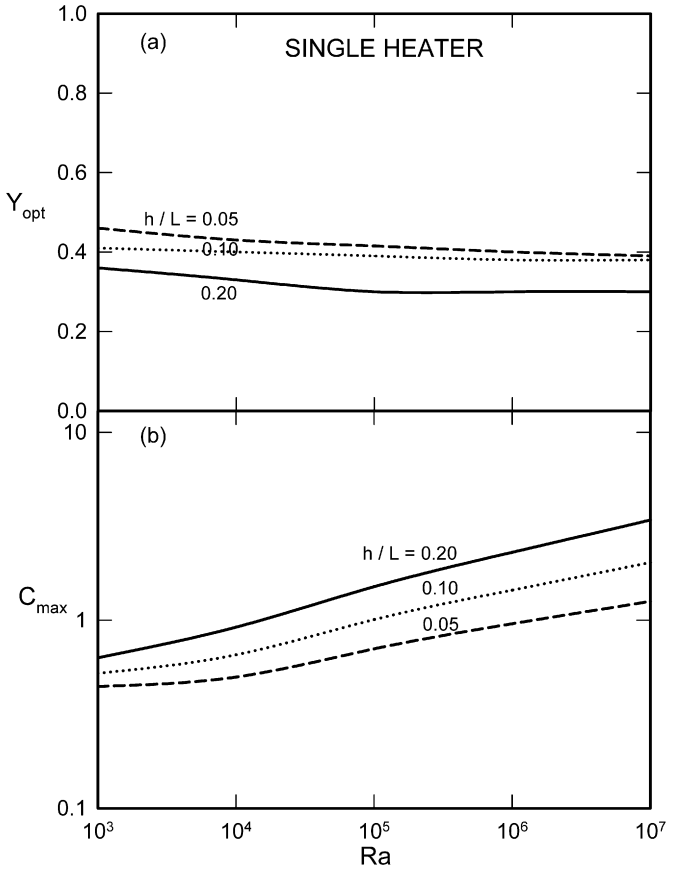

Fig. 4. (a) The optimal heater location and (b) corresponding maximum global conductance as a function of the Rayleigh number for the single heat source.

decreasing function of the Rayleigh for the same reason as explained earlier. Compared to the single heater case of Fig. 4, the first heater is at a lower level position and the second heater is at a higher level. We see in Fig. 5(b) that C_{max} is an increasing function of the Rayleigh as well as of h/L. Compared to a single heater case, we notice that C_{max} is generally increased since it is the global maximum conductance comprising two heaters.

We present the results with three heaters in Fig. 6. It appears in Fig. 6(a) that the optimum position Y_{opt} is again a decreasing function of Ra from 10^3 to 10^7 and also, it is a strong function of h/L from 0.05 to 0.20. We make similar observations regarding the positions of the heaters: when compared to the single and the two heaters cases, the first heater is at the lowest position and the third heater at the highest position. The maximum global conductance C_{max} presented in Fig. 6(b) is then function of the Rayleigh number and heater size, h/L. As in the previous two cases, the maximum global conductance is an increasing function of the Rayleigh number and also of the heater size h/L. We note also that the maximum global conductance C_{max} is increased with respect to the case of the two heaters of Fig. 5(b).

In comparison with the square enclosure case having $N = 1$, 2 and 3 [3], it is noted that the heater positions and distances between them have the expected trend at low Rayleigh numbers, a conduction dominated regime. At $Ra = 10^3$ for example, we compared the conductance results for $h/L = 0.10$ of Fig. 3

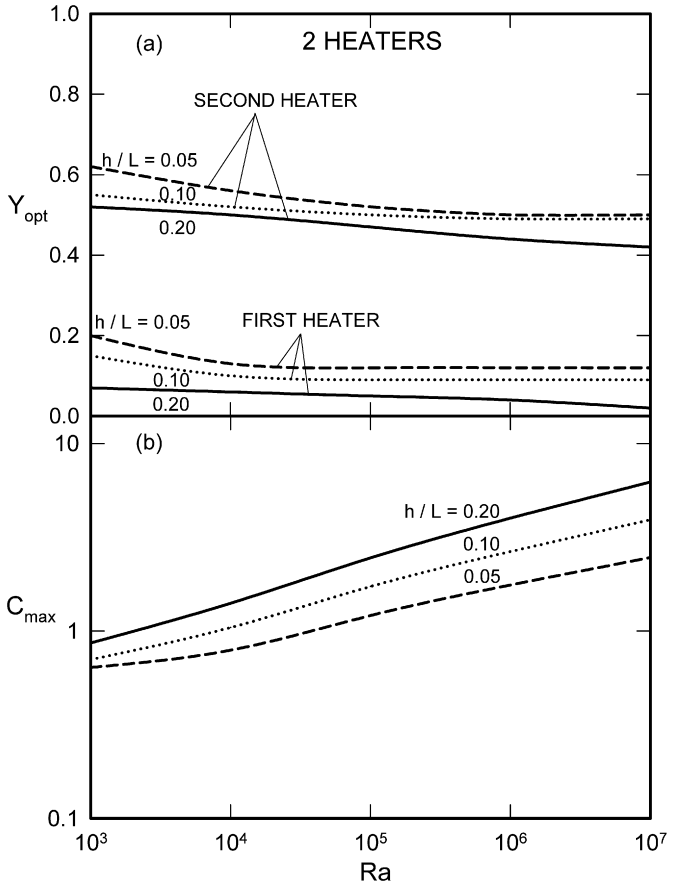

Fig. 5. (a) The optimal heater location and (b) corresponding maximum global conductance as a function of the Rayleigh number for two heat sources.

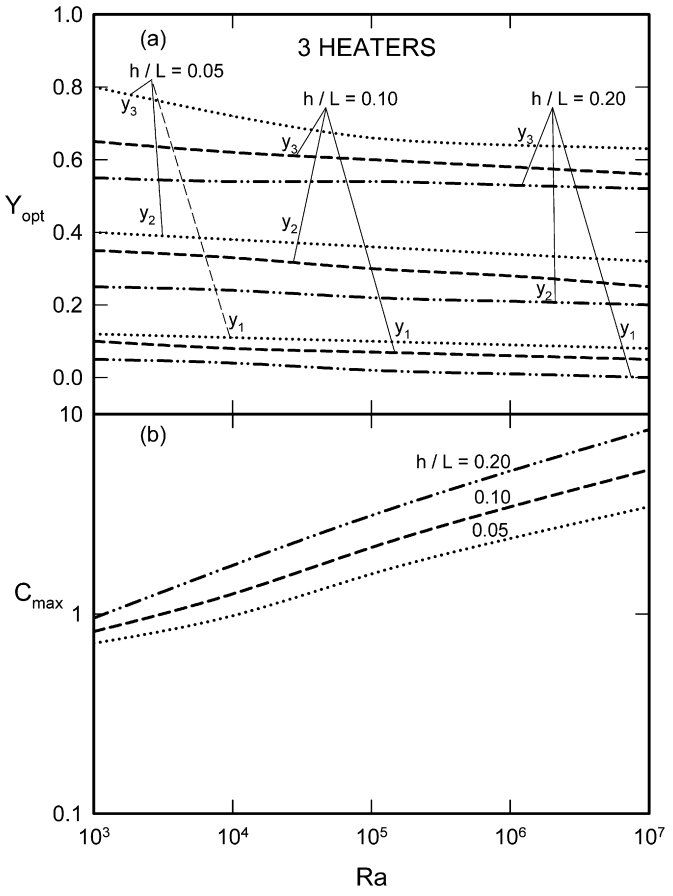

Fig. 6. (a) The optimal heater location and (b) corresponding maximum global conductance as a function of the Rayleigh number for three heat sources.

of [3] and found that the conductance in the open cavity was lower by 26.2%, thus showing that the cooling of the heater is quite different. Indeed, Y_{opt} in the open cavity case is lower by 2.5%, 9.2% and 8.5% for $h/L = 0.05$, 0.10 and 0.20 respectively. At high Rayleigh numbers, the heaters in the open cavity case are positioned at higher levels, although the overall positioning are similar: at $Ra = 10^6$ for example, Y_{opt} in the open cavity is positioned higher by 17.6%, 27% and 20% for $h/L = 0.05$, 0.10 and 0.20 respectively. In fact, the comparative iso-lines (not presented here) showed that the flow and temperature fields were quite different for enclosure and open cavity, particularly at high Rayleigh numbers. For example, at $Ra = 10^6$, in the enclosure case, $\psi_{\text{ext}}/\theta_{\max} = 7.4873$ ($X = 0.4125$, $Y = 0.5730$)/0.079 and in the open cavity case, $\psi_{\text{ext}}/\theta_{\max} = 11.5362$ ($X = 1.00$, $Y = 0.6620$)/0.069; the isotherms in the latter case showed that the temperature gradient was higher near the heater, thus heat transfer and cooling were more vigorous. The flow rate at the mid-plane ($X = 0.5$) of the enclosure and that at the exit plane of the open cavity are also quite different: $\dot{V}$ (enclosure)/$\dot{V}$ (open cavity) are 0.1363/0.2198 and 7.4345/11.5362 at $Ra = 10^3$ and 10^6 respectively. This is expected since the ambient air into the open cavity flows through the lower 2/3 part of the opening. In contrast, the air in the enclosure circulates close to the bottom wall, as a result of which the first heater's optimum position is closer to the bottom. We see that the flow and temperature fields in the enclosure and cavity cases are quite different. Thus, optimum positions are different, although some similarities exist, as they should.

4.2. Heat transfer and volume flow rate

The average normalized Nusselt number by Eq. (6) and the volume flow rate $\dot{V}$ by Eq. (7) are calculated and presented in Figs. 7 to 9 for the three cases of one, two and three heaters. The results are presented for the case of optimum positions, i.e. for the maximized conductance of each heater.

We present the case of single heater in Fig. 7. We see in Fig. 7(a) that *Nu* is an increasing function of *Ra* and h/L. At low Rayleigh numbers, the heat transfer is conduction dominated; *Nu* is equal to one for all three heater sizes. As *Ra* is increased the convection becomes dominant and we can see that *Nu* becomes an increasing function of the heater size h/L. The volume flow rate $\dot{V}$ as a function of *Ra* with h/L as a parameter is shown in Fig. 7(b). As expected, $\dot{V}$ is an increasing function of both *Ra* and h/L.

The case with the two heaters is shown in Fig. 8, which shows that the heat transfer is conduction dominated at $Ra = 10^3$, thereafter it becomes convection dominated. *Nu* is an increasing function of *Ra* and h/L. Compared to the single heater case for h/L from 0.05 to 0.20, *Nu* is increased by 15.6 to 7.8% respectively at $Ra = 10^7$ due to increased number of heaters. The volume flow rate $\dot{V}$ is also an increasing function of *Ra*

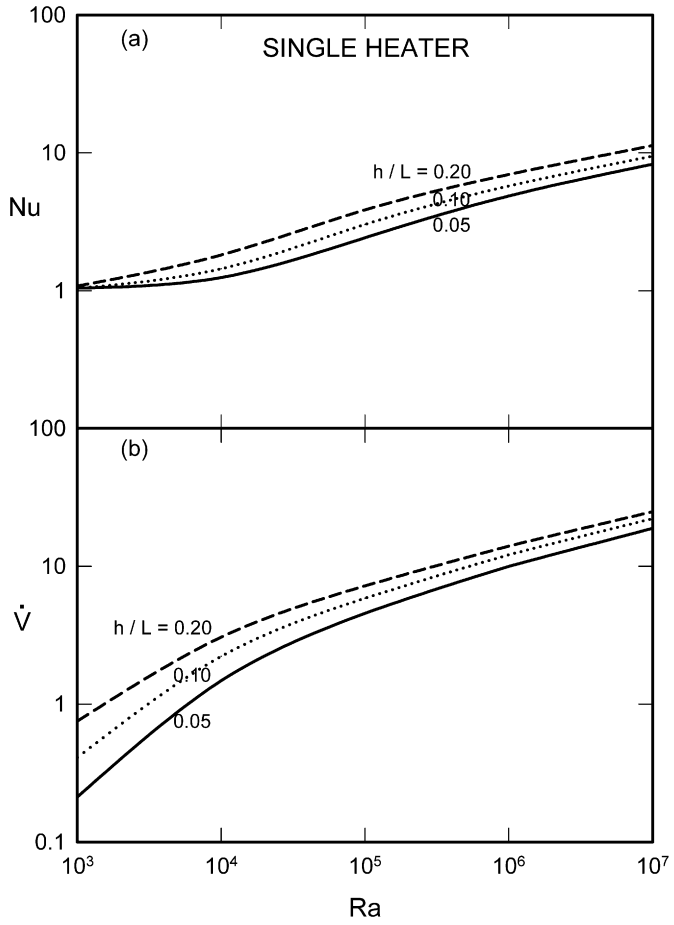

Fig. 7. (a) Nusselt number and (b) flow rate as a function of the Rayleigh number for the single heat source of three sizes.

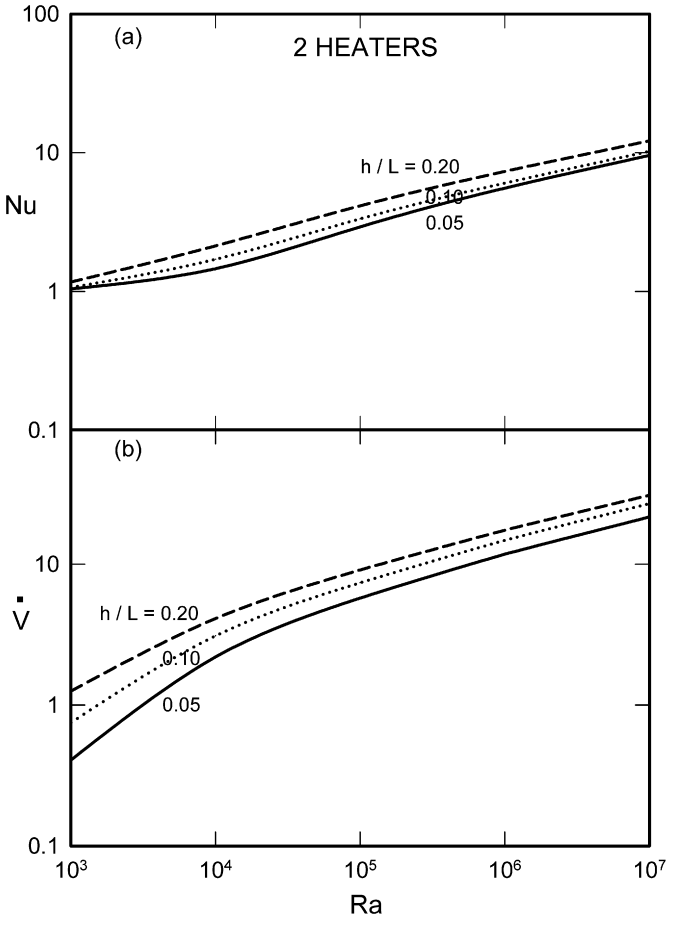

Fig. 8. (a) Nusselt number and (b) flow rate as a function of the Rayleigh number for the two heat sources of three sizes.

and h/L. Compared to the single heater case for h/L from 0.05 to 0.20, it is increased respectively by 91.8 to 67% at $Ra = 10^3$ and 15 to 24.4% at $Ra = 10^7$.

The case with three heaters is shown in Fig. 9. In this case also, both Nu and $\dot{V}$ are an increasing function of Ra and h/L. Fig. 9(a) shows that the heat transfer is in conduction regime at $Ra = 10^3$, thereafter it becomes convection dominated. Compared to the single heater case for h/L from 0.05 to 0.20, Nu is increased by 19.2 to 9.5% at $Ra = 10^7$. The flow rate $\dot{V}$ is increased by 1.77 to 1.17 times at $Ra = 10^3$ and by 29.9 to 40.9% at $Ra = 10^7$. Obviously, the changes of Nu and $\dot{V}$ are due to increased number of heaters.

To see the reason for increased heat transfer and volume flow rate with increasing heater number, the streamlines and isotherms for the case of $h/L = 0.10$ and $Ra = 10^6$ with one, two and three heaters at their optimum positions are produced and shown in Fig. 10. ψ_{ext} and $\theta_{\max}$ are 11.4124 ($X = 1$, $Y = 0.6625$) and 0.0691 respectively for the single heater case in Fig. 10(a). It is clearly seen that the heater is positioned at off center, at slightly lower part of the enclosure. The flow enters and moves upward following the position of the heater and flows over the vertical wall and top horizontal wall and exit as a jet. The cold ambient air enters at lower 2/3 of the opening section and the hot air exits at upper 1/3. The isotherms shown on the right hand side follow this trend as a consequence of which the air is cold in about 2/3 part of the cavity. For the two heater case in Fig. 10(b), the heaters are positioned with unequal distances from the enclosure bottom to the first heater and from the first to the second heater. ψ_{ext} and $\theta_{\max}$ are 14.7678 ($X = 1$, $Y = 0.6714$) and 0.0755 respectively. The strength of circulation is increased with respect to the single heater case. Since the optimum position of the first heater is at the lower part of the enclosure, the cold air enters and follows the bottom horizontal wall, heated at first by the first heater and then by the second, it flows over the whole vertical wall and exits following the top horizontal wall. The ambient air entrance section in this case is increased to 67.14% of the opening, which is little larger than 2/3. The isotherms shown on the right hand side of Fig. 10(b) depict clearly the domain of the cold air, which occupies the lower half of the enclosure. Compared to the single heater case, the air is heated by the first heater when the air reaches the vertical wall. Then by the second heater; then the air continues to go up, parallel to the vertical wall. The three heater case is shown in Fig. 10(c). In this case, the positions Y_{opt} are 0.05, 0.29 and 0.59 for the first, second and third heaters respectively, which correspond to the distance from the bottom to the first heater of 0.05 for the first heater, it is 0.14 between the first and second, and 0.20 between the second and third heaters. This clearly shows the optimum positioning of the three heaters with unequal distance between them. ψ_{ext} and $\theta_{\max}$ are in this case

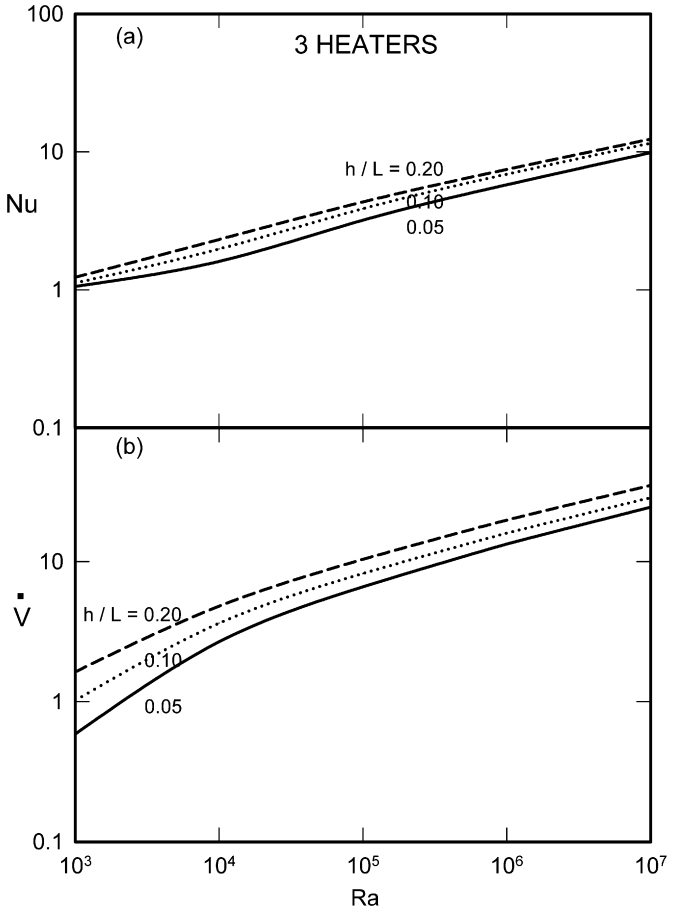

Fig. 9. (a) Nusselt number and (b) flow rate as a function of the Rayleigh number for the three heat sources of three sizes.

15.9682 ($X = 1$, $Y = 0.6875$) and 0.0873 respectively. As expected, the circulation is stronger with the three heater case with respect to the two heater case; otherwise, the appearance of the flow field is almost the same. The ambient air entrance section is further increased to 68.75% of the opening. The isotherms at the right hand side of Fig. 10(c) are with higher temperature gradients with respect to the case with two heaters; otherwise, they are similar.

5. Conclusions

We studied natural convection heat transfer in a square open cavity with discrete heat sources installed at the vertical wall facing the opening. The number of discrete heaters was from one to three; their size was varied from 0.05 to 0.20, and the Rayleigh number from 10^3 to 10^7. Conservation equations of mass, momentum and energy were solved by finite difference – control volume numerical method. At the beginning, the optimum positions of discrete heat sources were searched. Then, the heat transfer and volume flow rate were determined. In view of the results presented, the main points can be summarized as follows.

For best thermal performance of discrete heaters installed on the vertical wall facing the opening of a square cavity, the optimum positioning is not uniform with equidistance between them. The optimum positioning is obtained by maximizing the

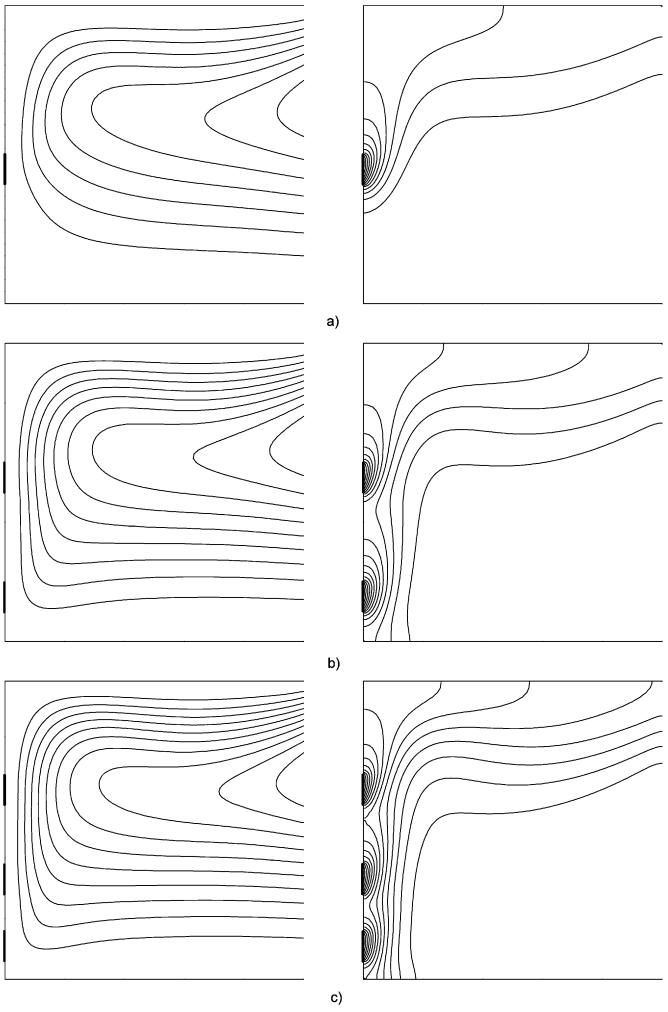

Fig. 10. Streamlines (on the left) and isotherms (on the right) with $h/L = 0.10$ and $Ra = 10^6$. (a) One heater at its optimum position, $Y_{opt} = 0.38$, (b) two heaters at their optimum positions, $Y_{opt} = 0.09$ and 0.49, (c) three heaters at their optimum positions, $Y_{opt} = 0.06$, 0.28 and 0.58.

global performance. The heaters are positioned closer to each other at the beginning of the fluid flow. The final configuration of discrete heaters depends on Rayleigh number.

The maximum global conductance is quasi-independent of Rayleigh number for single and double heaters and $h/L = 0.05$ at $Ra < 10^4$. The maximum global conductance is strongly Rayleigh number dependent in other cases; it increases with increasing Rayleigh number. Similarly, the maximum global conductance is increased with the number of heaters as well as with the heater size.

In determining the maximum conductance, we observe broad optima in C versus Y plots; in practical terms, this does not cause any difficulty in determining C_{max}. On the other hand, it shows that there is certain flexibility for positioning of the heaters if the technical circumstances require it.

At low Rayleigh numbers, $Ra < 10^4$, it is conduction dominated regime. At higher Rayleigh numbers, the convection becomes dominant regime. Generally, the Nusselt number and the volume flow rate are increasing function of the Rayleigh number, the heater size and the number of discrete heaters.

Acknowledgements

The financial support for this study by Natural Sciences and Engineering Research Council Canada is acknowledged.

References

[1] H.Y. Wang, F. Penot, J.B. Sauliner, Numerical study of a buoyancy-induced flow along a vertical plate with discretely heated integrated circuit packages, Int. J. Heat Mass Transfer 40 (1997) 1509–1520.
[2] Y. Liu, N. Phan-Thien, An optimum spacing problem for three chips mounted on a vertical substrate in an enclosure, Numer. Heat Transfer A 37 (2000) 613–630.
[3] A.K. da Silva, S. Lorente, A. Bejan, Optimal distribution of discrete heat sources on a wall with natural convection, Int. J. Heat Mass Transfer 47 (2004) 203–214.
[4] A.K. da Silva, S. Lorente, A. Bejan, Optimal distribution of discrete heat sources on a plate with laminar forced convection, Int. J. Heat Mass Transfer 47 (2004) 2139–2148.
[5] A.K. da Silva, S. Lorente, A. Bejan, Maximal heat transfer density in vertical morphing channels with natural convection, Numer. Heat Transfer A 45 (2004) 135–152.
[6] A.K. da Silva, G. Lorenzini, A. Bejan, Distribution of heat sources in vertical open channels with natural convection, Int. J. Heat Mass Transfer 48 (2005) 1462–1469.
[7] A.K. da Silva, L. Gosselin, Optimal geometry of L and C-shaped channels for maximum heat transfer in natural convection, Int. J. Heat Mass Transfer 48 (2005) 609–620.
[8] O. Polat, E. Bilgen, Conjugate heat transfer in inclined open shallow cavities, Int. J. Heat Mass Transfer 46 (2003) 1563–1573.
[9] S.V. Patankar, Numerical Heat Transfer and Fluid Flow, Hemisphere Publishing Corporation, New York, 1980.
[10] E. Bilgen, R. Ben Yedder, Natural convection in enclosure with heating and cooling with sinusoidal temperatures on one side, Int. J. Heat Mass Transfer 50 (2007) 139–150.
[11] D. de Vahl Davis, Natural convection of air in a square cavity: a benchmark solution, Int. J. Numer. Methods Fluids 3 (1983) 249–264.
[12] D.C. Wan, B.S.V. Patnaik, G.W. Wei, A new benchmark quality solution for the buoyancy driven cavity by discrete singular convolution, Numer. Heat Transfer B 40 (2001) 199–228.
[13] Y.L. Chan, C.L. Tien, A numerical study of two-dimensional natural convection in square open cavities, Numer. Heat Transfer 8 (1985) 65–80.